



<http://go.asme.org/HPVC>

## Vehicle Description Form

(Form 6)

Updated 12/3/13

### Human Powered Vehicle Challenge

Competition Location: San Jose, California

Competition Date: April 24-26, 2015

***This required document for all teams is to be incorporated in to your Design Report. Please Observe Your Due Dates; see the ASME HPVC for due dates.***

#### Vehicle Description

School name: Olin College of Engineering  
Vehicle name: Llama Del Rey  
Vehicle number 9

#### Vehicle configuration

Upright \_\_\_\_\_ Semi-recumbent X  
Prone \_\_\_\_\_ Other (specify) \_\_\_\_\_

Frame material Carbon Fiber-Aluminum Monocoque

Fairing material(s) Carbon Fiber

Number of wheels 3

#### Vehicle Dimensions (please use in, in<sup>3</sup>, lbf)

Length	<u>94.7 in</u>	Width	<u>31.0 in</u>	
Height	<u>43.5 in</u>	Wheelbase	<u>39.4 in</u>	
Weight Distribution	Front <u>60%*</u>	Rear	<u>40%*</u>	Total Weight <u>TBD**</u>
Wheel Size	Front <u>16 in</u>	Rear	<u>20 in</u>	
Frontal area	<u>920 in<sup>2</sup></u>			
Steering	Front <u>X</u>	Rear	_____	
Braking	Front <u>X</u>	Rear	_____	Both <u>_____</u>
Estimated Cd	<u>0.089</u>			

Vehicle history (e.g., has it competed before? where? when?) Llama del Rey was designed exclusively for the 2015 ASME HPV Challenge and has not yet competed.

---

\* Vehicle has not been completed, weight distribution estimated.

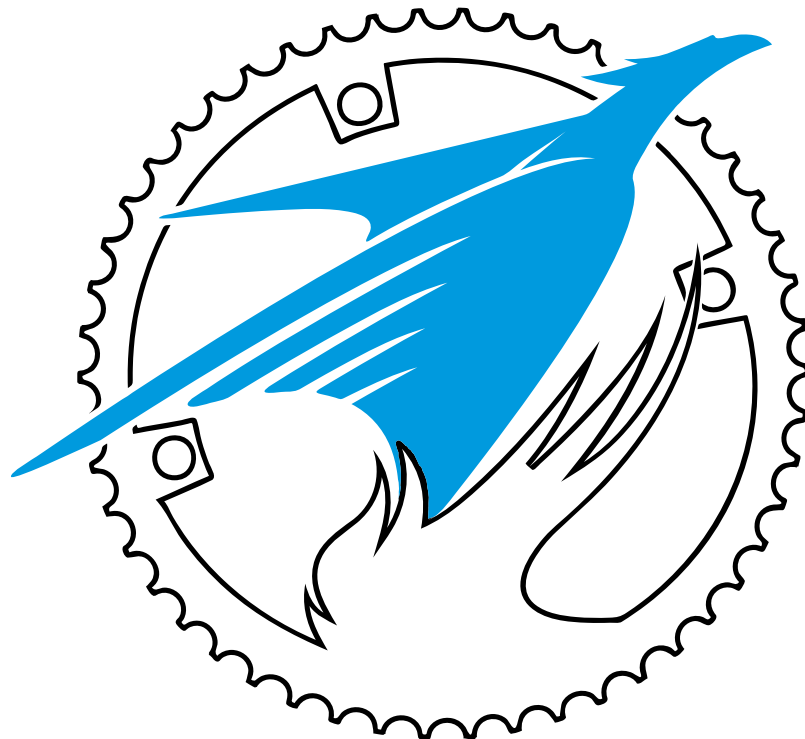
---

\*\* Expected weight is 64lbf.



**Olin College Human Powered Vehicles**  
OF ENGINEERING

## 2014 - 2015 Design Report



## Llama Del Rey Vehicle #9

Alex Spies	Anisha Nakagawa	Becca Getto	Cullen Ross
Charlie Mouton	David Pudlo	Dennis Chen	Gaby Waldman-Fried
Halley Pollock-Muskin	Ingrid Hagen-Keith	Janie Harari	Jay Patterson
Jennifer Wei	Jessica Sutantio	Josh Sapers	Kari Bender
Kevin Crispie	Kristyn Walker	Lucy Wilcox	Maddie Fort
Maggie Jakus	Maggie Su	Mary Ruthven	Mike Warner
Morgan Bassford	Nagy Hakim	Nick Eyre	Paul Titchener
Shrinidhi Thirumalai	Shruti Iyer	Tatiana Anthony	Zarin Bhuiyan

*Faculty Advisors:*  
Aaron Hoover & Christopher Lee

hpv@olin.edu    <http://hpv.olin.edu>

8

7

6

5

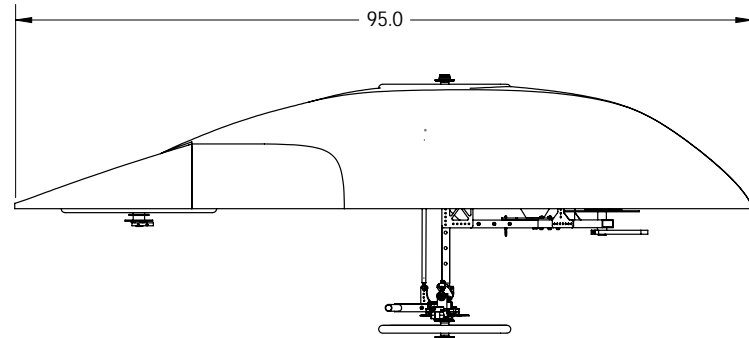
4

3

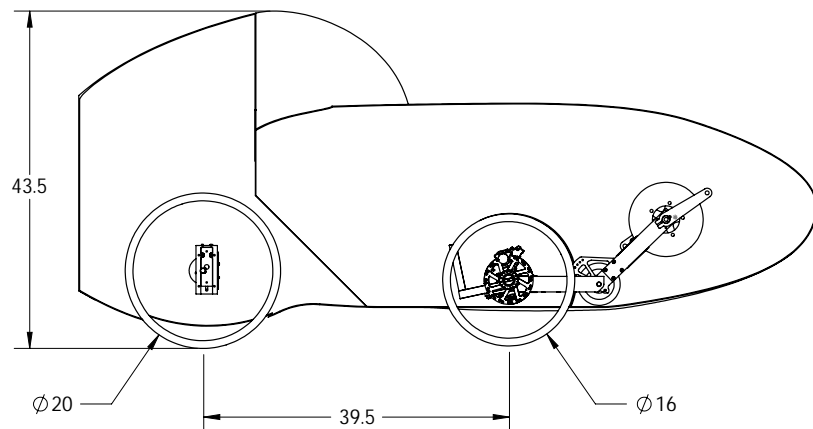
2

1

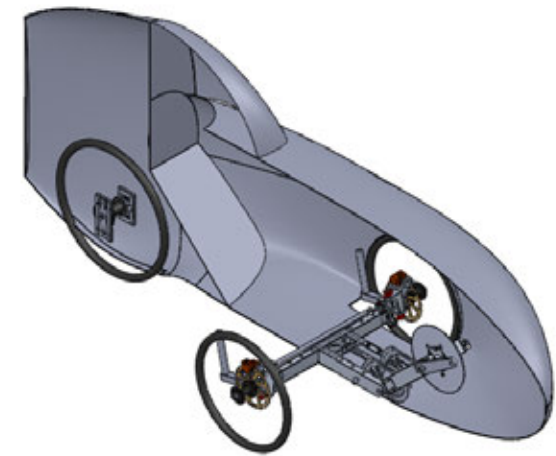
D



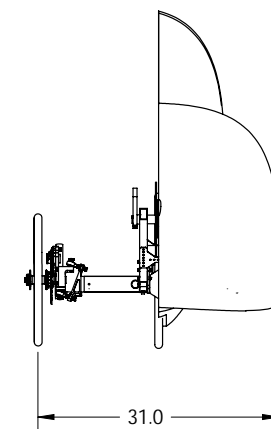
C



B



A



8

7

6

5

4

3

2

1

UNLESS OTHERWISE SPECIFIED:	
DIMENSIONING AND TOLERANCING PER ASME Y14.5M-1994	PERPENDICULARITY: $\perp$ 0.001° / INCH
DIMENSIONS ARE IN INCHES	CENTRICITY: $\bigcirc$ 0.002° T.I.R.
DEBURR AND BREAK ALL SHARP EDGES .003 MIN.	PARALLELISM: // 0.001° / INCH
TOLERANCES ARE: X.X = ± 0.2 X.XX = ± 0.01 X.XXX = ± 0.005 ANGLES: ± 0.5°	FLATNESS: □ 0.001° / INCH ROUGHNESS: 125/ 125/
THIS DRAWING IS THE SOLE PROPERTY OF THE FRANKLIN W. OLIN COLLEGE OF ENGINEERING HUMAN POWERED VEHICLE DESIGN TEAM. DO NOT DUPLICATE WITHOUT PERMISSION	
INITIAL DRAWN CHECKED	DATE 3/19/2015 3/20/2015
ENGINEER TEAM N. EYRE	SIZE PART NO. OLIN-HPV2015
REV A	SCALE 1:16 DO NOT SCALE PRINT SHEET 1 OF 1

 Olin College of Engineering  
Human Powered Vehicles

Llama Del Rey

2015 COMPETITION VEHICLE



## Abstract

This year, the Olin College Human Powered Vehicle Design Team returns to the ASME Human Powered Vehicle Challenge with its new vehicle, *Llama Del Rey*. This year's vehicle builds upon last year's practical and reliable design with the goal of increasing its competitive performance and safety qualities. Following the team's long-standing tradition, the vehicle is built to accommodate all team members. The team's performance at the 2014 competition led the team to focus on the following areas:

1. *Llama Del Rey* will be a safe vehicle. *Llama*'s stability, maneuverability, and excellent rider vision will help riders avoid crashes. The successful integrated seat-rollbar from the 2014 vehicle will return in tandem with improved Nomex-honeycomb ribs to maintain the vehicle's structural integrity in the case of any crashes.
2. *Llama Del Rey* will be a stable vehicle at all speeds. As a tricycle, *Llama* will be inherently stable when static but will also corner at high speeds with its refined Ackerman steering. High stability and maneuverability will be advantageous for endurance event obstacles and will be easy for all riders to use.
3. *Llama Del Rey* will be lighter and more aerodynamic than the 2014 competition vehicle. *Llama*'s aluminum frame, minimalist rear wheel mounting and superior strength-to-weight fairing construction allow for 10 lbs to be eliminated from the previous year's design. Eliminating the outboard wheels and optimizing the shape will reduce aerodynamic drag by 35%.
4. *Llama Del Rey*'s fairing will be manufactured using a two-part male-mold process to reduce labor, eliminate internal lay-ups, and increase strength through better adhesion between carbon layers.



# Contents

<b>I Design</b>	<b>1</b>
<b>1 Objective</b>	<b>1</b>
<b>2 Background</b>	<b>1</b>
<b>3 Prior Work &amp; Background Research</b>	<b>1</b>
<b>4 Organizational Timeline</b>	<b>1</b>
<b>5 Design Specifications</b>	<b>2</b>
<b>6 Vehicle Configuration</b>	<b>3</b>
<b>7 Structural Monocoque Fairing</b>	<b>4</b>
7.1 Structural Design . . . . .	4
7.2 Aerodynamic Design . . . . .	4
7.3 Rollover Protection System . . . . .	5
7.4 Manufacturing Process . . . . .	6
<b>8 Drivetrain</b>	<b>7</b>
<b>9 Sub-Frames</b>	<b>7</b>
<b>II Analysis</b>	<b>8</b>
<b>10 Rollover Protection System Analysis</b>	<b>8</b>
<b>11 Aerodynamic Analysis</b>	<b>9</b>
<b>12 Structural Analysis</b>	<b>11</b>
12.1 Front Frame . . . . .	11
12.2 Knuckle Components . . . . .	13
12.3 Adjustable Pedal Components . . . . .	14
12.4 Pedal Adjustment Pins . . . . .	14
12.5 Rear Wheel Mounting . . . . .	15
<b>13 Other Analyses</b>	<b>15</b>
13.1 Speed & Gearing Analysis . . . . .	15



13.2 Rollover Analysis . . . . .	16
<b>14 Cost Analysis</b>	<b>17</b>
<b>III Testing</b>	<b>18</b>
<b>15 Rollover Protection System Testing</b>	<b>18</b>
<b>16 Developmental Testing</b>	<b>20</b>
16.1 Prone Position Testing . . . . .	20
16.2 Automatic Shifting . . . . .	20
16.3 Fairing Size Verification . . . . .	20
16.4 Fairing Manufacturing Tests . . . . .	21
16.5 Frame Structural Testing . . . . .	22
16.6 Rib Testing . . . . .	22
<b>17 Performance Testing</b>	<b>24</b>
17.1 Weight Testing . . . . .	24
17.2 Visibility Testing . . . . .	24
17.3 Turning Radius . . . . .	25
17.4 Center of Mass . . . . .	25
17.5 Handling Testing . . . . .	25
17.6 Rider Changeover . . . . .	26
<b>IV Safety</b>	<b>26</b>
<b>18 Design for Safety</b>	<b>26</b>
<b>19 Hazard Analysis</b>	<b>28</b>
<b>20 Safety in Manufacturing</b>	<b>28</b>
<b>V Conclusion</b>	<b>29</b>
<b>21 Comparison</b>	<b>29</b>
<b>22 Evaluation</b>	<b>29</b>
<b>23 Recommendations</b>	<b>30</b>



# Part I

# Design

## 1 Objective

For the 2014-2015 season, the Olin College of Engineering Human Powered Vehicles Team iterated on the previous year's tricycle design with the goals of increasing aerodynamic performance, improving rider vision, and reducing fairing fabrication time. All these qualities were achieved while maintaining excellent stability, maneuverability, and ease-of-use. This year's vehicle was also designed to have more torsional stiffness, better chain routing, and reduced weight.

## 2 Background

Global climate change and the increasing cost of fossil fuels have inspired communities worldwide to invest in more environmentally friendly forms of transportation. While bicycles are convenient and economical, they lack the safety features and speed offered by automobiles. Faired recumbents offer increased rider protection and power efficiency unparalleled by traditional bicycles, making them a good alternative to modern automobiles.

## 3 Prior Work & Background Research

*Llama Del Rey* borrows its core configuration from *Cheryl*[5], Olin's 2014 competition vehicle, but also implements key features from other past vehicles. This year's tunable Ackerman steering system is a refinement of the 2014 solution, allowing for greater ease of adjustment. While the pivoting adjustable pedals are a new feature for the team, custom crank design and chain management techniques for rear-wheel drive vehicles are drawn from our 2014 and 2011 vehicles. *Llama*'s rear wheel mounting system is the next iteration in a series of increasingly minimal solutions that have evolved since 2012. The integrated seat-rollbar makes its second appearance after being developed for the 2014 vehicle.

This year, the team used the Rickey Horwitz Design Primer[7] heavily in the design of the steering geometry, using his specific definitions of steering geometry components to optimize our handling characteristics. Component friction data from Friction Facts[3] was also used in the selection of drivetrain components, indicating the advantage of larger derailleur sprockets and influenced our derailleur selection. Furthermore, the team drew inspiration from numerous vehicles in the ASME Human Powered Vehicles Competition including those built by previous Olin teams. Finally, the team's mold manufacturing techniques were inspired by those of the University of Toronto's Human Powered Vehicle Team[9].

## 4 Organizational Timeline

*Llama* was designed and constructed entirely in the spring 2015 semester by a team of 32 students at the Olin College of Engineering. The team began the semester by designing



Week of	Design		Manufacture		Testing
	Fairing	Drivetrain	Fairing	Drivetrain	
26-Jan	Shape	Drivetrain			
2-Feb		Steering			Fairing Manufacture
9-Feb	Ribs	Frame			
16-Feb			Mold Making	Machining	Frame
23-Feb			Composite Lay-Up		
2-Mar				Assembly	
9-Mar				System Integration	RPS Test
16-Mar			Hatches		
23-Mar			Window		Full Vehicle
30-Mar				Spare Parts	
6-Apr					
13-Apr			Ship Vehicle		
20-Apr			Competition		

Figure 1: Organizational timeline.

the vehicle in three weeks, using analysis and testing of past vehicles to drive the iterative design process (Figure 1). The majority of February and March was devoted to vehicle construction. Finally, in late March and early April, the vehicle was tested and shipped to competition. While the vehicle was constructed in a short period of time, it built on developmental testing and experience that has accumulated over the team's ten years.

## 5 Design Specifications

A house of quality was used to move from the team's desires for the vehicle to concrete specifications which could be used in its design (Figure 2). In the house, desires are located on the left and capabilities are listed along the top. The body of the house contains values indicating the strength of correlations between the two to aid in capability prioritization. The roof of the house details how improving one aspect of the vehicle affects other aspects.

Key design desires prioritized by the team included rider safety, ease of construction, reliability, speed, performance, and ability for all riders to operate the vehicle. The house of quality identified key areas of prioritization including roll bar strength and responsive handling.

From the house of quality and the ASME HPVC rules, the team created a list of concrete and measurable design specifications that could be used to guide the design of *Llama Del Rey* (Table 1).

Specification	Target
Roll bar vertical strength	600 lbf
Roll bar lateral strength	300 lbf
Turning radius	3 m
Weight	65 lb
Drivetrain efficiency	95%
Repair time	20 min
Vehicle construction time	350 hrs
Vehicle width	32 in
Vehicle length	92 in
Drag coefficient ( $C_d A$ )	0.05
Cost of materials	\$2,500
Rider changeover time	60 sec
Field of View	200°
Number of parts	50
Stopping distance (15 mph)	20 ft
Cargo area can fit grocery bag	
Responsive handling	
Rider safety harness present	
No sharp edges near rider	
Aesthetically pleasing vehicle	

Table 1: Vehicle specifications.

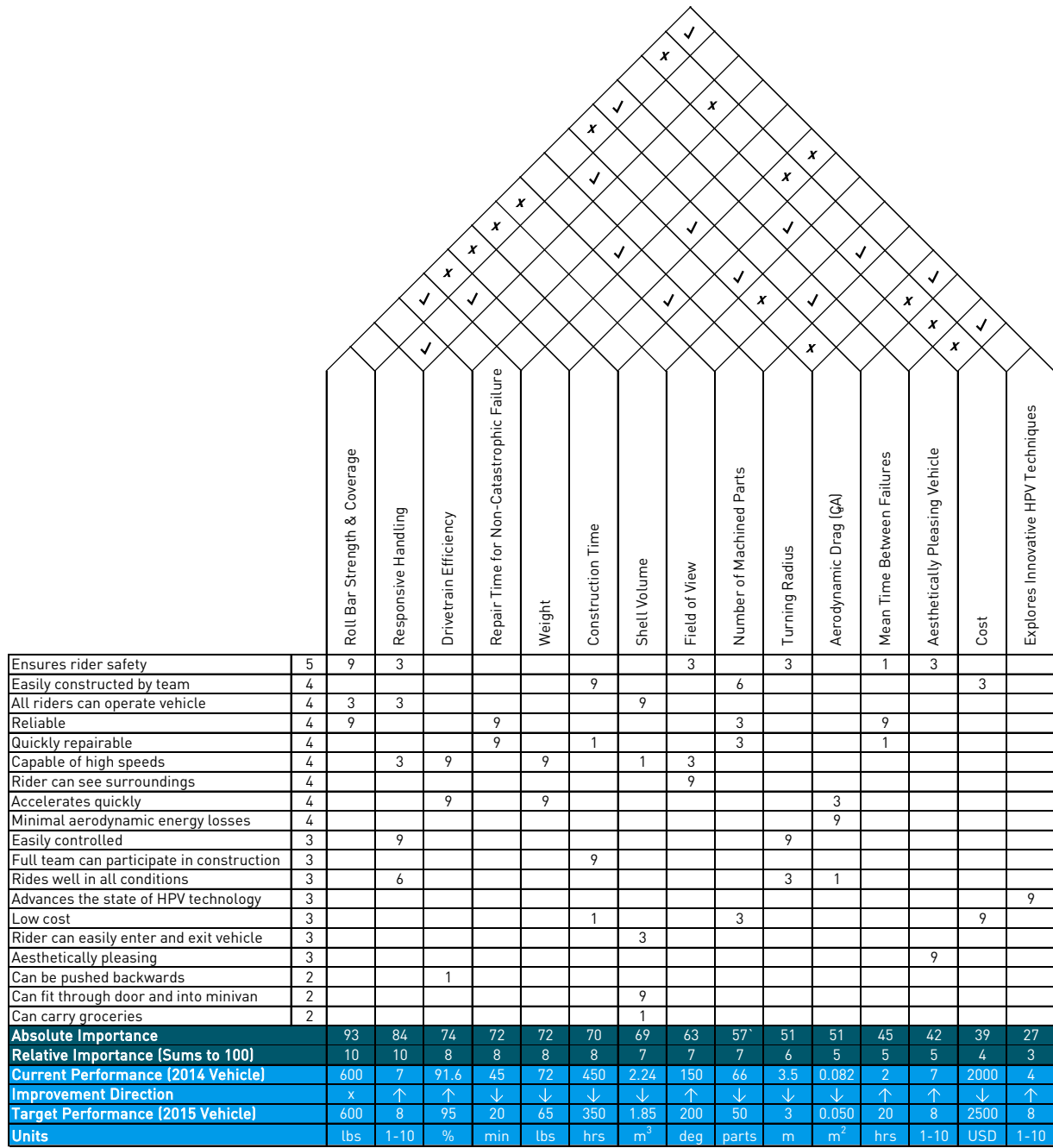


Figure 2: House of quality.

## 6 Vehicle Configuration

In 2014, the team used a design matrix to decide on a tadpole tricycle layout based on the team's priorities of stability, maneuverability, and ease-of-use. The tadpole's performance in each of these categories was confirmed at the 2014 competition. As the team's priorities have not substantially shifted, a faired tadpole tricycle was again selected. *Cheryl*'s high aerodynamic drag and poor visibility were addressed when designing *Llama*. The 2015 vehicle improves on its predecessor by narrowing the front track width, placing the wheels in cut-outs flush to the fairing's surface, and raising the rider's head above the fairing's front. By iterating upon a proven design with these performance-improving architectural



changes, *Llama* will be a fast, efficient, and practical vehicle.

## 7 Structural Monocoque Fairing

### 7.1 Structural Design

*Llama* is built as a ribbed carbon fiber monocoque shell with aluminum sub-frames. The monocoque shell is structural and acts as the rollover protection system, keeping the rider safe in the event of a crash. The main body of the vehicle is composed of two layers of 6K twill weave carbon fiber. Ribs have an additional 0.5" thick Nomex honeycomb core with lightweight polyurethane foam along their edges.

The team decided on this structural paradigm after considering several options in a weighted design matrix (Figure 3). The most highly weighted criteria in the analysis were rider safety, weight, fairing quality, and composites manufacturing time. From this analysis, the team determined that a carbon monocoque with an integrated rollover protection system best met the team's design criteria. Although producing this structure is time consuming, the result has a high strength to weight ratio.

This structure is also advantageous in that it is easy to bolt metal sub-frames into the thick laminated honeycomb ribs. All drivetrain and steering components are mounted to the modular front sub-frame, which can be removed for maintenance. The rear wheel is independently supported by aluminum plates that interface with ribs in the monocoque.

### 7.2 Aerodynamic Design

*Llama*'s fairing shape is designed to reduce drag by closely enclosing the rider and wheels in an airfoil-like profile. After an initial model was created, computational fluid dynamics simulation was used to iterate upon the design and optimize the form.

In order to maximize visibility, the rider's head is fully enclosed in a clear PET plastic windshield, ensuring more than 200° of visibility. Furthermore, the vehicle features a fixed seat back to ensure that all riders' heads are in the same place relative to the window. A seat angle of 37° was chosen as the lowest angle that would allow for sufficient peripheral and frontal vision.

This year, the tricycle's front wheels are flush with the sides of the monocoque (Figure 4). The exposed wheels allow for quick maintenance and repair, which the team has found to be necessary with past vehicles. Although the wheel holes may negatively affect the aerodynamics of the vehicle, it was determined that this was a better option than increasing the frontal area to enclose the wheels. The fairing width is less than 32", meeting the desired design specification.

	Weight	Carbon Monocoque & Roll Bar	Carbon Monocoque, Steel Roll Bar	Steel Frame, Structural Fairing	Steel Frame, Non-Structural Fairing
Rider Safety	10	10	9	7	2
Weight	8	8	6	0	2
Repairability	4	0	2	4	4
Interface Complexity	6	5	0	3	3
Schedule Complexity	6	2	0	4	4
Time - Composites	8	2	2	4	6
Time - Welding	4	4	2	0	0
Fairing Quality	8	8	8	6	4
Total		72%	54%	52%	46%

Figure 3: Structure design matrix.



Figure 4: *Llama Del Rey's* aerodynamic fairing.

*Llama's* fairing was designed for improved ingress and egress for all riders. A large hatch is cut around the rider's head, allowing for easy access to the rider cavity. Ribbed handholds on either side of the hatch sit flush with the vehicle and provide structural points which the rider can use as handles when entering and exiting. Finally, the vehicle has a hatched compartment above the rear wheel to allow for grocery and cargo storage. Both hatches are held onto the structural monocoque with magnets placed around their perimeters.

### Alternatives Evaluated

Alternative fairing designs were centered around different front wheel or window designs.

Three schemes were considered for front wheel analysis: completely inboard wheels, faired outboard wheels (similar to *Cheryl*) and hybrid flush wheels. Flush wheels were chosen as a good balance between aerodynamic efficiency and vehicle width.

For the window design, the team considered a fully enclosed head, a fully exposed head, and a hybrid design with an exposed head with optional window. The final design was chosen to balance aerodynamics, visibility, and rider comfort during extended use.

### 7.3 Rollover Protection System

*Llama* contains the team's fourth iteration of the integrated composite fairing rollover protection system (RPS). In past years, the RPS has consisted of a hoop of carbon fiber covering a wide foam rib with horizontal steel support tubes. Last year was the first year that the seat was integrated into the roll bar structure, allowing for a continuous composite laminate across the rear of the RPS and eliminating the need for lateral support tubes. This integration decreased weight and increased strength.

This year, 1/2" thick, 1/8" cell-width Nomex honeycomb was used as the rib and seat material. This is stronger and lighter than the polystyrene ribs of years past. Kevlar was placed around the rider to prevent carbon splintering in the case of catastrophic failure.



*Llama's* RPS is the strongest and lightest the team has built to date.

## 7.4 Manufacturing Process

This year, the team developed a two-cavity male mold manufacturing process inspired in part by the University of Toronto HPVT [9]. This novel process completely eliminated internal layups and simplified manufacturing, resulting in a stronger monocoque. Furthermore, rib precision was enhanced by cutting all ribs into the original male mold.

**Mold:** *Llama's* mold was machined on a CNC router from 3" thick slices of extruded polystyrene (XPS) insulation foam. The slices were aligned with dowels and joined with epoxy to form two large plugs: one for the front and one for the rear of the vehicle. The plugs were assembled in vacuum bags to ensure that the slices were flush against one another. The plugs were sanded, and plaster was used to fill any gaps. Finally, the molds were painted in epoxy and coated in Loctite Frekote mold sealant.

**Seat Layup:** Kevlar was applied to the mating surface of the front plug to form the seat back (bulkhead wall) and the top surface of the back plug to form the head rest. The Kevlar was also placed around all other surfaces surrounding the rider cavity.

**Rib Filling:** Nomex honeycomb was cut to size and tightly set into the ribs with epoxy. Gaps were filled with two-part expanding polyurethane foam. The surface was then faired (Figure 5b).

**Joining & Outer Shell:** After a layer of honeycomb was applied to the mating surface of the rear plug, the two fairing halves were aligned and bonded (Figure 5a). Epoxy and carbon were placed between the two halves to fill minute gaps between the sections. Carbon was then applied to the mold, with additional layers around the perimeter of the mating surface.

**Male Mold Extraction:** Hatches were cut through the center of strategically placed ribs, and the foam male mold was cut out through these hatches.

**Sub-Frame Mounting:** The front frame and rear wheel mount plates were aligned in the fairing and mounted with screws and washers.

**Finishing:** Filling compound was used to fill dents and imperfections in the outer surface of the shell. The fairing was then faired and painted.

**Window:** The window was made from 0.04" thick PET using a vacuum forming machine.

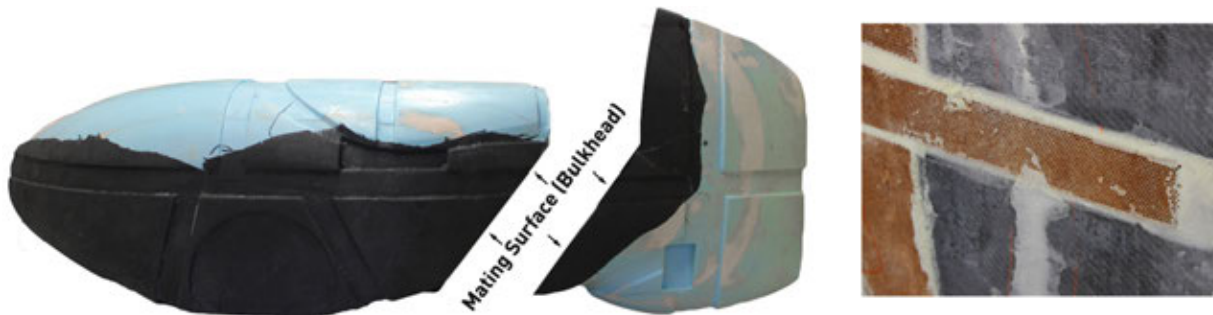


Figure 5: Two male molds covered in first carbon layer (left) and filled and faired ribs (right).



## 8 Drivetrain

*Llama Del Rey* is a rear-wheel drive vehicle with an interchange near the crankset. A rear-wheel drive was chosen to avoid a differential on the front wheels.

This year, the team has incorporated several design changes to improve performance. *Llama's* chain runs under the vehicle's body to reduce chain friction and improve repairability. A traditional rear derailleur is mounted at the front interchange, and shifting occurs on the front chain. This design ensures that the rear chain does not change length and allows for a narrower rear cavity (Figure 6).

*Llama* adjusts for rider position with a swing-arm-based adjustable pedal system (Figure 7). This system allows all riders to ride the vehicle while keeping riders' heads located within a compact window. Previous adjustable pedal systems in the team's 2012 and 2013 vehicles used a four-bar linkage to constrain the pedals. This year, a swing arm was designed to adjust pedal position (Figure 7). The swing arm is simpler to manufacture than the linkage-based design and reduces the system part count.

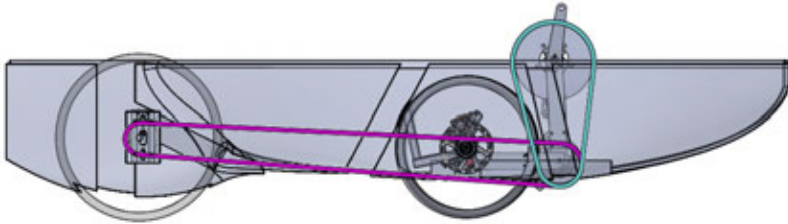


Figure 6: Chain routing.



Figure 7: Adjustable pedal mechanism (left and center) and interchange detail (right).

## 9 Sub-Frames

Components are held to the monocoque with two 6061-T6 aluminum sub-frames. The front frame (Figure 7a) mounts to a large laminate rib and supports the front wheels and adjustable pedal assembly.

The rear wheel is supported by two aluminum sliding plate assemblies that are secured with clamping bolts. These plates allow for shaft alignment: one allowing for adjustment in the vertical direction, and the other in the horizontal direction.



## Part II

# Analysis

### 10 Rollover Protection System Analysis

**Objective:** Ensure that the vehicle's composite rollover protection system (RPS) will keep the rider safe if the vehicle rolls over.

**Method:** Analysis was performed in SolidWorks Simulation 2014. The monocoque fairing was modeled using surface elements to determine deformation under load. Ribbed regions of the fairing (Figure 8) were modeled using the experimentally determined modulus of the carbon-honeycomb test specimens (Developmental Testing Section 16.6). Non-ribbed regions were modeled using experimentally determined values for two laminated layers of 6k carbon twill weave. This modeling simplifies the composite structure as a linear and isotropic homogenous material. Although carbon fiber reinforced polymers do not generally exhibit these properties, testing demonstrated that these are valid assumptions for the expected loading.

Two simulations were conducted. In both, the monocoque was constrained at the base of the seat. In the first, a 600 lbf load was applied to the top of the vehicle at an angle 12° from vertical. Next, a 300 lbf side load was applied to the side of the vehicle at shoulder level. Both of these represent the inertial loads of the vehicle falling.

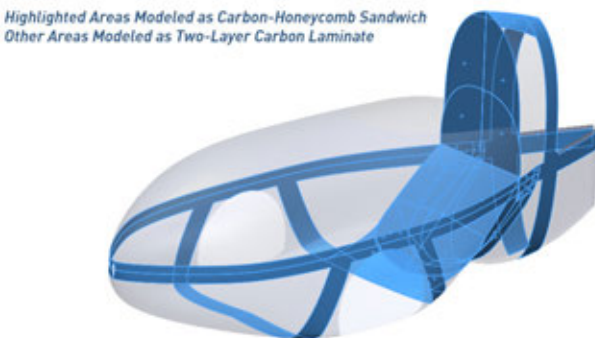


Figure 8: RPS ribs.

	Load	Max. Deflection
Top Load	600 lb	0.47 in
Side Load	300 lb	0.32 in

Table 2: RPS analysis results.

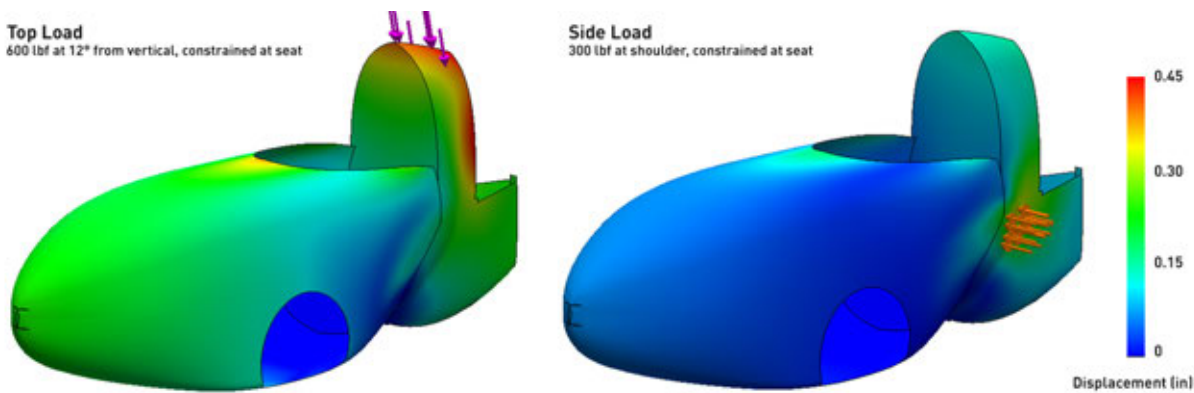


Figure 9: Rollover protection system structural analysis results.

**Results:** Under the top load, a maximum deformation of 0.47 inches is experienced at the top of the monocoque. Under the side load, the fairing undergoes a maximum deformation



of 0.32 inches at the shoulder (Table 2). The deformation of the fairing under both loading cases is shown in Figure 9.

**Impact on Design:** This analysis indicates that the rollover protection system designed for *Llama Del Rey* will keep the rider safe in a severe crash with a significant factor of safety. This implies that the design of *Llama* will meet the desired specifications and no further design changes are necessary.

## 11 Aerodynamic Analysis

**Objective:** Use computational fluid dynamics (CFD) modeling tools to guide the iterative design of an aerodynamic vehicle.

**Method:** CD-adapco's STAR-CCM+ CFD simulation software was used to simulate the aerodynamic performance of *Llama Del Rey* and compare it to past vehicles. The simulations assume a forward vehicle speed of 30 mph and include a moving ground surface under the vehicle. Including ground effects increases the accuracy of the measurements and prevents drag coefficient inflation. One notable simplification is that the wheels are modeled as solid non-rotating bodies. Though this affects the results, it is consistent with past years' analyses and allows for comparison between years. In a separate simulation, the effects of a 10 mph crosswind from the left were simulated.

The simulation was configured with a  $k-\epsilon$  turbulence model to represent the effects of turbulent flows on the vehicle. Convergence was determined by monitoring the continuity and momentum residuals. Drag forces were determined by numerically integrating both the pressure and shear force gradients over the surface of the vehicle in the direction of interest. The parameter that matters most in the design of an aerodynamic shape is  $C_dA$ , the drag coefficient multiplied by the frontal area.  $C_dA$  can be calculated from the drag force. A lower value of  $C_dA$  indicates a more aerodynamic shape.

**Results:** The final vehicle fairing shape has a  $C_dA$  value of 0.053, much lower than the 2014 vehicle's 0.082 value (Table 3). Note that although the 2012 and 2013 vehicles have even lower  $C_dA$  values, these two vehicles are bicycles, not tricycles, and have a substantially reduced frontal area. The drag coefficient of *Llama* is comparable to that of *Seabagel*.

	Head-On		Crosswind	
	$F_D$ (N)	$C_dA$ ( $m^2$ )	$C_d$	$F_D$ (N)
<b>2015 Fairing - 1<sup>st</sup> Iteration</b>	24.0	0.218	-	-
<b>2015 Fairing - 2<sup>nd</sup> Iteration</b>	18.0	0.163	-	-
<b>2015 Fairing - 3<sup>rd</sup> Iteration</b>	6.47	0.059	-	-
<b><i>Llama Del Rey</i> (2015 Final)</b>	<b>5.83</b>	<b>0.053</b>	<b>0.089</b>	<b>410</b>
<i>Cheryl</i> (2014)	8.98	0.082	0.185	307
<i>The Plaid Panther</i> (2013)	3.60	0.033	0.094	331
<i>Seabagel</i> (2012)	3.94	0.036	.0870	283

Table 3: Aerodynamic analysis results and comparison to past vehicles.

The aerodynamic differences between *Llama* and *Cheryl* can be further visualized by looking at the wake velocity profiles behind the vehicles (Figure 10). Note that the column of disturbed air behind the 2015 vehicle converges much faster than that of the 2014



vehicle. Additionally, *Cheryl*'s outboard wheels further disturb the flow. The reduced air disturbance behind *Llama* gives the 2015 vehicle a substantial aerodynamic advantage over *Cheryl*.

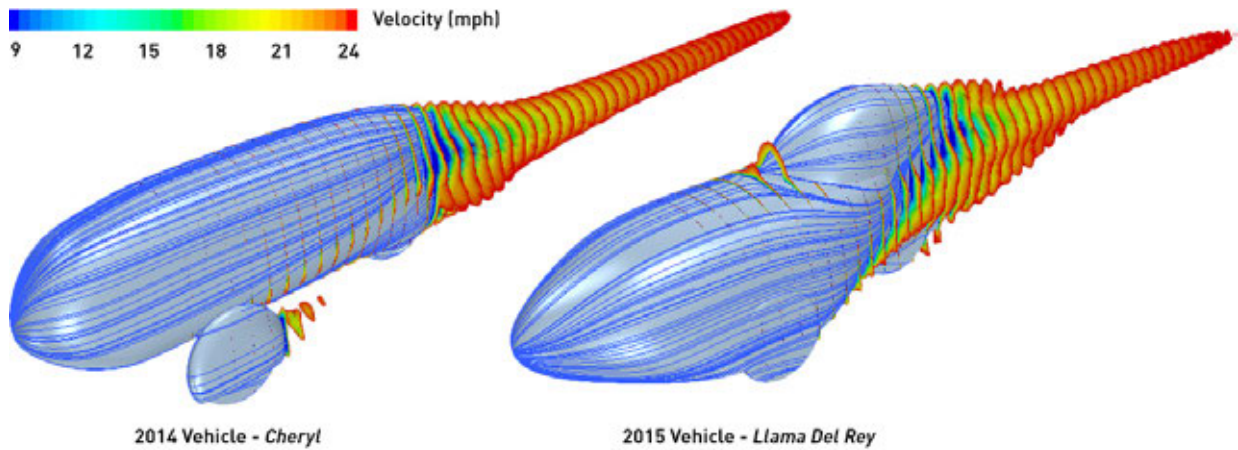


Figure 10: Head-on aerodynamic simulation results. Colored regions indicate reduced flow velocity in vehicle wake.

In a crosswind, *Llama* is not as aerodynamic as its predecessors. In a 10 mph crosswind, the 2015 vehicle is resisted by 410 N of sideways drag force, much greater than *Cheryl*'s 307 N. In a tricycle, a crosswind moment is reacted against the outboard wheels and the lateral friction force on the ground. Given these results, the team is confident that the vehicle will not roll over or break traction due to a 10 mph crosswind. Furthermore, the team has not had issues in the past with handling during a crosswind, so the team believes that increased crosswind drag will have negligible effects on race performance. The crosswind flow profiles are shown in Figure 12.

**Impact on Design:** The design of *Llama*'s aerodynamic shell was an iterative process guided by quick feedback from CFD simulation. Over the course of this year's fairing design process, several iterations were tested (Figure 11). For each, streamlines on the surface were used to identify spots of high flow disruption and velocity profiles were used to pinpoint regions of the fairing that cause large flow speed reductions.

The results of the CFD simulation allowed the team to see improvements that could be made. For example, the aerodynamic simulation results early on pointed out the necessity of a window. Doing so would help guide flow around the rider's head and consequently, a window was incorporated into the final vehicle design.

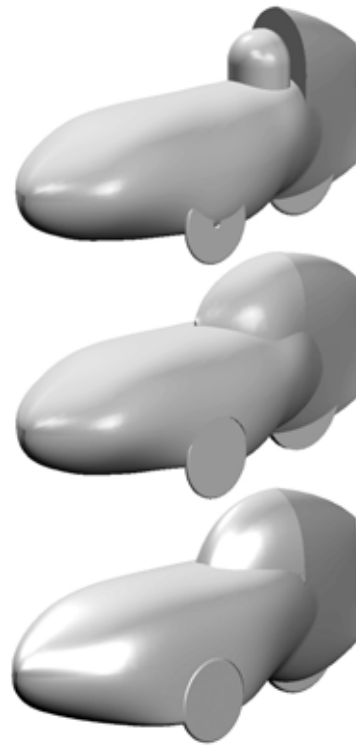


Figure 11: From top: initial fairing concept, concept 3, and final design.

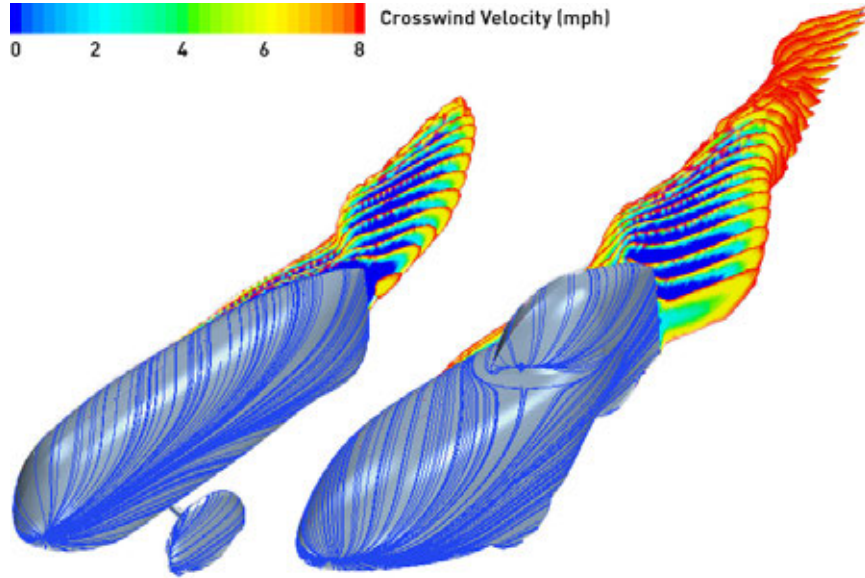


Figure 12: Crosswind simulation results. Colored regions indicate reduced flow velocity.

## 12 Structural Analysis

### 12.1 Front Frame

**Objective:** Ensure that the front frame and its connections to the monocoque will not fail under expected loads.

**Model & Assumptions:** The frame was geometrically simplified for analysis (Figure 13a). At points  $L$ ,  $R$  and  $N$ , the fairing is held into the vehicle by bolts. The frictional force  $F_{Fric}$  is generated by the normal force of the polyurethane rubber between the metal frame and the carbon monocoque. The number of mount points was reduced to create a statically determinate system, leading to load overestimates at the mount points.

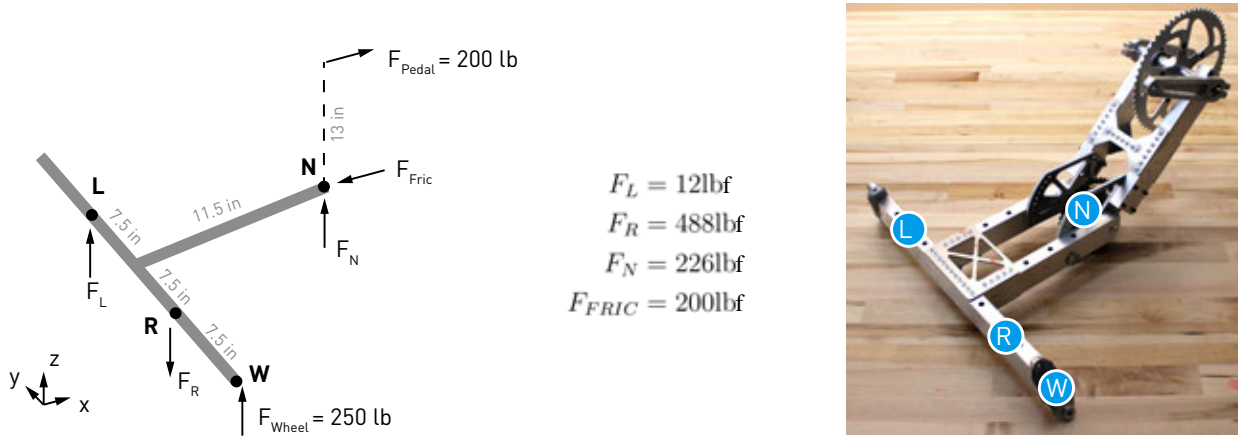


Figure 13: Front frame structural model (a), resultant forces (b) and front frame (c).

External forces include a 200 lbf pedaling force and a 250 lbf wheel force. This is a worst-case analysis and assumes that the entire weight of the vehicle is up on one wheel while



the rider is pedaling. The resultant forces on the mounting points were determined by balancing the forces and moments of the system (Figure 13b).

**Bolt Strength:** The sub-frame is held into the vehicle with #10-32 socket head cap screws which pass through fender washers and into the carbon-honeycomb laminate. The Nomex honeycomb has a compressive strength of 85 psi and the bolts will be preloaded to 75% of the honeycomb's strength (50 lbs).

The alloy steel socket head cap screws have a minimum rated tensile strength of 170 ksi or 3400 lbs calculated at the bolts' tensile stress area[4]. This preload, combined with the worst case bolt tensile load of 488 lbf at point  $F_R$  gives a sizable safety factor of 7.

**Mounting Point Strength:** The bolts and washers passing through the honeycomb laminate apply a bending and shear load on the floor of the monocoque. A finite element simulation was conducted in SolidWorks Simulation using the modulus and yield strength of the laminate as tested (Section 16.6). A 488 lb load representative of  $F_R$  was applied on a washer-sized region of the bottom of the monocoque. The structure was constrained at the seat. The maximum deformation was 0.1" and minimum safety factor was 2.4. This simulation gives the team confidence that the monocoque will not fail at these mounting points.

**Frictional Requirements:** The pedaling force and moment on the front frame is counteracted in part by the frictional force on either side of the polyurethane rubber sheet ( $F_{FRIC}$ ). The frictional force is generated both by reaction force  $F_N$  and by the preload on the six bolts in this region. Assuming dry Coulomb friction, a coefficient of friction of  $\mu_S = 0.38$  is required to oppose the pedaling force. If the coefficient of friction is lower than this, the frame will shift and the mounting bolts will be placed in shear. The expected coefficient of friction of the 60A durometer polyurethane used is approximately 0.5[8], giving a factor of safety (FoS) of 1.3.

**Frame Strength:** Hand calculations were performed on both beams of the modeled front frame to determine the maximum normal bending stress. Calculations showed that under the expected loading, the maximum bending stresses are 5.7 ksi on the transverse beam and 7.9 ksi on the longitudinal beam. Both of these values are significantly less than the 6061-T6 tube's yield strength of 40 ksi, indicating that the front frame will not fail. Finite element analysis confirmed that the bending stresses are much lower than the material strength and suggest that the material surrounding the nuts on the lower tube has a lower, but still permissible, factor of safety of about 1.5.

**Impact on Design:** The results of these analyses were used in several places throughout the design process. The analysis supported the choice of #10-32 fasteners as a sufficiently strong mounting option. The thickness of the monocoque underneath the frame was influenced by analysis results. The urethane rubber under the frame was chosen to have an acceptably high coefficient of friction. Frame strength analysis suggested that while most of the frame may be overbuilt, the areas around the embedded nuts are weak points and should not be aggressively lightened.



## 12.2 Knuckle Components

**Objective:** Ensure that the critical components of the knuckle assembly do not fail under worst-case loading conditions.

**Model & Assumptions:** The knuckle, knuckle mount, and front wheel shaft were all simulated for a static and a worst case tipping scenario. The static case consists of a downward force of 125 lbs representative of the vehicle and rider weight, while the tipping case simulates all 250 lbs of vehicle weight tipping up on one wheel 10° from vertical.

The brake and caliper mount pieces were subjected to a rapid braking load to simulate coming to a complete stop from 30 mph in two seconds using a single brake. The remote load (Equation 1) was applied at the brake pad contact patch.

$$F = 7m/s^2 * \frac{250\text{lbf}}{9.8m/s^2} = 175\text{lbf} \quad (1)$$

Solidworks Simulation finite element analysis was used to simulate the loads on the knuckle components. All components were constrained at the point where they interfaced with the vehicle frame. Remote loads were used to simulate the forces and moments of wheel loading. All parts are modeled as 6061-T6 aluminum except for the front wheel shaft, which is instead made from 7075-T6 aluminum.

**Results:** Under worst-case loading, all components have factors of safety greater than one (Figure 14). Deformation on all parts was minimal. These results give confidence that *Llama*'s knuckle components will support the necessary front wheel loads.

**Design Modifications:** These results identified that some components of the knuckle assembly are severely overbuilt and may benefit from design modification. In particular, the brake mount pieces and the knuckle body will be investigated for weight reduction.

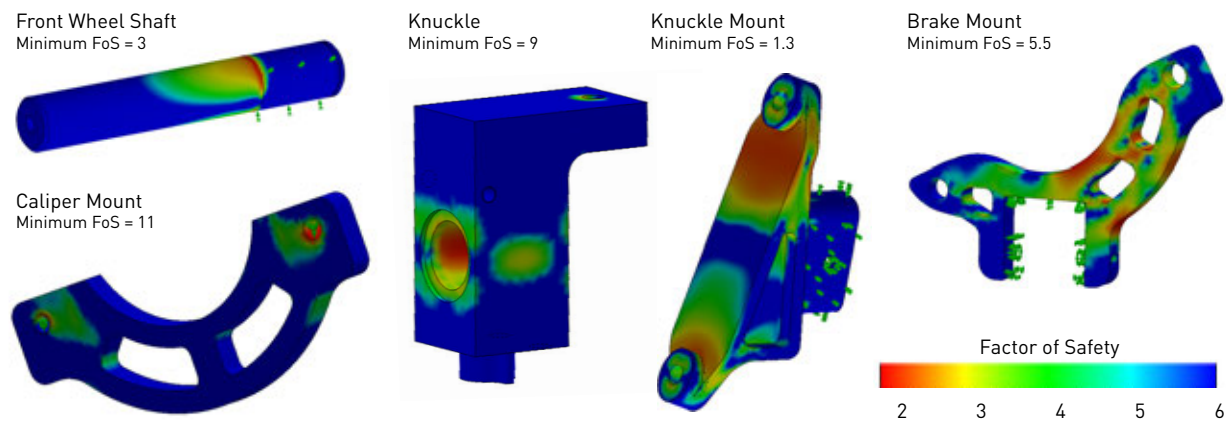


Figure 14: Knuckle component structural analysis results.



### 12.3 Adjustable Pedal Components

**Objective:** Ensure that the critical components of the adjustable pedal assembly do not fail.

**Model and Assumptions:** In the worst-case loading scenario, the rider is pushing with full force on a single pedal, estimated at 200 lbf. Finite element analysis was used to simulate the loads on the adjustable pedal components. All parts were loaded with remote loads representing the applied forces and moments. All parts are made of 6061-T6 aluminum except for the 7075-T6 crankshaft. Simulation was performed in SolidWorks.

**Results:** Both the swingarm plates and the crankshaft were analyzed and were found to have a FoS of 1.2 (Figure 15). The cranks had a FoS of 1.6 and the chainring hub had a FoS of 2.5. These safety margins suggest that even under worst case loading, the adjustable pedal components will not fail.

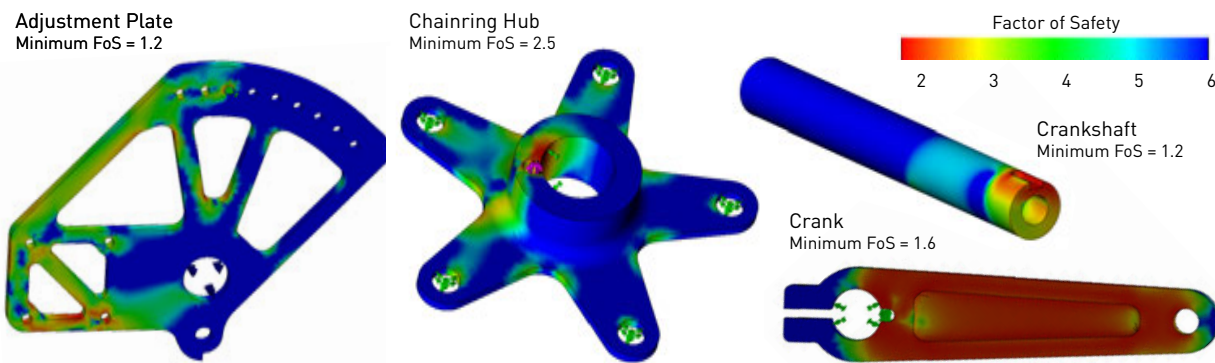


Figure 15: Results of adjustable pedals component structural analysis results.

**Impact on Design:** Analysis demonstrated that many of the components in the pedal assembly are not substantially overbuilt and may need a material change if additional lightening is to be pursued. The team plans on investigating alternative materials for maintaining strength and stiffness at reduced weight.

### 12.4 Pedal Adjustment Pins

**Objective:** Ensure that the pedal adjustment pin holes will not be damaged by loads exerted by the rider.

**Method:** The moment on the adjustment swing arm was balanced to determine the reaction force at the pins (Figure 16). Bearing force on the tubes at the pins was calculated.

**Results:** The bearing stress on each wall of the tube was calculated to be 10.4 ksi, much lower than the 40 ksi material yield strength.

**Impact on Design:** Due to the high factor of safety at these holes, this area will not need reinforcement if the frame tube walls are made thinner.

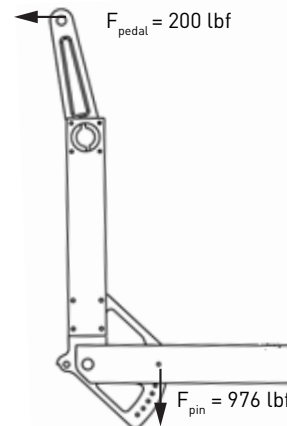


Figure 16: Adjustment pin loading.



## 12.5 Rear Wheel Mounting

**Objective:** Ensure that the adjustable rear-wheel mounting assembly will not fail under load.

**Loading:** *Llama's* final weight with rider is estimated to be 250 lbs with 40% of the weight on the front wheel. Using SolidWorks Simulation, a 150 lbf load was placed on the rear wheel shaft. The rear wheel shaft is held by two adjusting plates which are clamped in place.

**Clamping Screws:** The weight of the vehicle is transferred to the monocoque through friction between clamped plates. The 1/4-20 socket head clamping screws have a minimum rated tensile strength of 170 ksi. Assuming dry Coulomb friction, a coefficient of friction of  $\mu_s = 0.2$ , and that the four bolts are preloaded to 75% of their yield strength, the rear wheel is secured with 3200 lbf of frictional force. This yields a factor of safety of 21.

**Component Structural Analysis:** Finite element analysis was run on the assembly in Solidworks 2014. The minimum simulated factor of safety was 11, indicating that the mount plates will not fail (Figure 17).

**Conclusions & Impact on Design:** Analysis showed that the rear wheel mounting assembly is sufficiently strong. Lightening will be explored in future weeks.

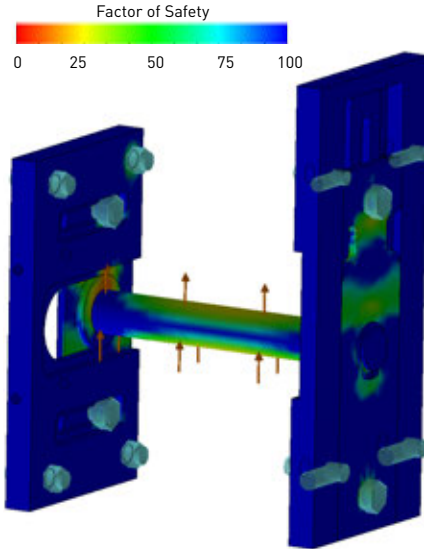


Figure 17: Rear wheel mounting structural analysis results.

## 13 Other Analyses

### 13.1 Speed & Gearing Analysis

**Objective:** Ensure that *Llama's* gearing allows the rider to reach maximum performance, given the constraints of the vehicle.

**Method:** The team used a dynamic analysis of the vehicle system to determine the maximum vehicle speed at a certain power input given weight and aerodynamic drag[6]. From last year's rider power testing data, the team estimates that our most powerful rider can sustain 300 W in a sprint. At 300 W, *Llama's* estimated top speed is 40 mph.

Shifting Sprockets			Speed (mph)			Fixed Sprockets		
Speed	Teeth	Total Ratio	70 rpm	90 rpm	110 rpm	Chainring	60 teeth	
			Cadence	Cadence	Cadence	Interchange Out	34 teeth	Rear Wheel Sprocket
1	34	3.0	12.5	16.1	19.6			
2	24	4.3	17.7	22.8	27.8			
3	22	4.6	19.3	24.8	30.3			
4	20	5.1	21.2	27.3	33.4			
5	18	5.7	23.6	30.3	37.1			
6	16	6.4	26.6	34.1	41.7			
7	14	7.3	30.3	39.0	47.7			

System Parameters	
Drive Wheel Diameter	20 inch

Table 4: Gearing analysis.

To pick vehicle gear ratios, the team used a spreadsheet to calculate bike speed for



given sprocket sizes and rider cadences: 70 rpm, 90 rpm and 110 rpm (Table 4).

**Results:** Analysis suggests that the ideal shifting cassette for *Llama* has a range of 14 to 38 teeth. This would allow the vehicle to reach its maximum speed while also providing sufficient gearing for easy acceleration, low-speed maneuvering, and hill climbing.

**Impact on Design:** A 14-34 cassette was chosen for *Llama*. Unfortunately, the team was not able to source a freewheeling cassette with a larger low speed cog. The chosen cassette has most of its cogs in the high speed range, supporting acceleration as per the analysis.

### 13.2 Rollover Analysis

**Background:** The house of quality (Figure 2) identified that reducing vehicle width would be beneficial for aerodynamics and practicality (i.e. fitting through doors).

**Objective:** Determine how changes in wheelbase affect vehicle stability while turning.

**Method:** As the vehicle turns, the normal force on the outer wheel is reduced until a critical point when the wheel lifts up. To determine liftoff velocity, the gravitational moment and the induced moment from centripetal acceleration were balanced about an axis between the two wheels on the inner side of the turn (Figure 18a). Friction vectors coincide with this axis and do not induce a moment.

This balance results in an equation for maximum velocity on a curve ( $V$ ) which is dependent on turn radius ( $r$ ), gravitational acceleration ( $g$ ), the location and height of the center of mass ( $d, h$ ), and the dimensionless ratio of wheelbase width and length ( $w/l$ ) (Equation 2). The vehicle center of mass with a rider was determined by leaning the vehicle to its balancing point and measuring the angle.

$$V = \sqrt{\frac{wrgd}{2hl}} \quad (2)$$

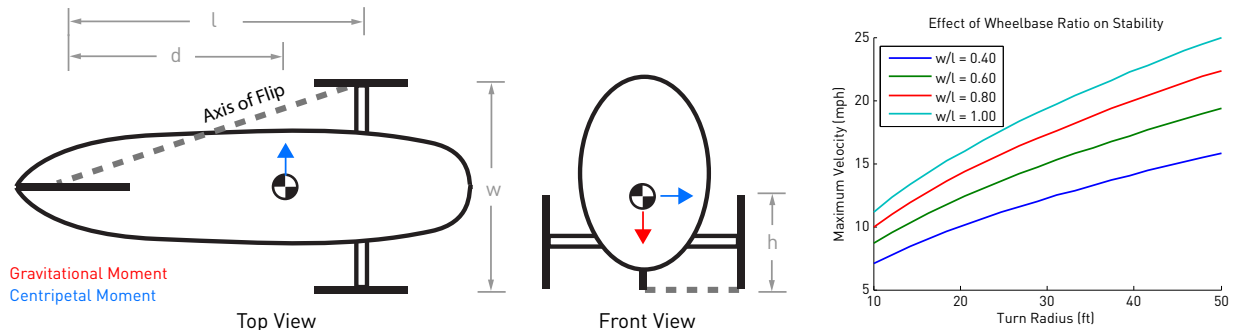


Figure 18: Rollover analysis method (a) and results (b).

**Results & Discussion:** A parameter sweep of wheelbase ratios was used to determine the ideal ratio ( $w/l$ ) for stability at a given speed and turn radius (Figure 18b). To traverse the competition's approximately 20 ft radius turns at 10 mph, a ratio of 0.4 is sufficient. A larger ratio allows for higher speed turns.

**Impact on Design:** Based on these results, *Llama* was designed to have a shorter wheelbase length and width, with a ratio of 0.78, slightly more stable than *Cheryl's* 0.73 ratio. These dimensions will reduce wheel lift up, which was an occasional problem with *Cheryl*.



on downhill turns, and also allow the vehicle to be narrower.

## 14 Cost Analysis

Both the cost of producing *Llama Del Rey* as presented and the expected cost of a three year production run are shown in Table 5.

**Comparison to Specification:** *Llama*'s material cost of \$2770 exceeds the \$2500 cost specification. This is primarily due to a higher than expected cost for the extruded polystyrene foam and the composite fabrics used to produce the mold and the monocoque. In retrospect, the specification was not realistic given the vehicle's desired capabilities and the team's suppliers.

**Production Run:** Production cost estimates are made assuming a three-year production run of ten vehicles per month, including labor costs and equipment capital investment. A bulk purchase savings of 40% on parts and raw materials is assumed. At production scale, each vehicle is estimated to cost about \$5100 to produce.

**Income:** Funding for the team's activities was provided by our generous sponsors (Table 6).

	Cost	Subtotal	Totals
<b>Material Cost</b>			
<b>Commercial Off-the-Shelf Parts</b>		\$ 825	
Steering System	\$ 170		
Drivetrain System	\$ 370		
Brake System	\$ 200		
Fastening Hardware	\$ 85		
<b>Metal &amp; Plastic Stock</b>		\$ 245	
Aluminum Square Tubing	\$ 25		
Aluminum Stock	\$ 190		
Steel Plate	\$ 30		
<b>Composites &amp; Supplies</b>		\$ 1,700	
Composites Fabrics	\$ 640		
Epoxy System	\$ 120		
XPS Foam	\$ 640		
Vacuum Bagging Supplies	\$ 300		
<b>Single Vehicle Material Cost</b>		\$ 2,770	
Production Bulk Materials Discount		40%	
<b>Production Vehicle Materials Cost</b>		\$ 1,662	
<b>Monthly Production Costs</b>			
<b>Labor per Vehicle</b>		\$ 2,800	
Machinist	\$ 1,600		
Composite Technician	\$ 1,000		
Assembly Technician	\$ 200		
<b>Overhead per Month</b>		\$ 1,650	
Rent	\$ 1,200		
Utilities	\$ 400		
Machine Upkeep	\$ 50		
<b>Total Monthly Production Costs</b>		\$ 29,650	
<b>Production Line Capital Investment</b>			
CNC Router	\$ 18,000		
CNC Mill	\$ 45,000		
Lathe	\$ 25,000		
Water Jet Machine	\$ 80,000		
Welder	\$ 4,000		
Vacuum Pump	\$ 350		
Hand Power Tools	\$ 1,200		
<b>Total Capital Investment</b>		\$ 173,550	
<b>36 Month 360 Vehicle Production Run</b>			
<b>Total Cost</b>		\$ 1,839,270	
<b>Cost per Vehicle</b>		\$ 5,109	

Table 5: Cost estimate for *Llama* as built and for a 360 vehicle, 3 year production run.

Team Funding Source	Amount
Corporate Donations	\$ 6,700
Grants	\$ 2,050
Family & Alumni Donations	\$ 6,075
<b>Total Income</b>	\$ 14,825

Table 6: Team income during 2014-2015 competition season.



## Part III

# Testing

## 15 Rollover Protection System Testing

**Objective:** Ensure that *Llama Del Rey's* composite monocoque is sufficiently strong to protect the rider in the event of a serious crash.

### Top Load

**Method:** The monocoque was subjected to a 600 lbf top load applied above the rider's head at 12° from vertical. The load was applied using an Instron mechanical tester (Figure 19). The vehicle was constrained by straps at the seat; the region of the monocoque directly opposing the applied load was not supported.

The compressive load was applied at a rate of 0.5 in/min through a piece of expanded polystyrene foam, distributing the load across an approximately 10 in<sup>2</sup> region. After reaching 630 lbf, 5% above the required specification, the load was held, the fairing was inspected for damage and deformation was measured. The load was relaxed and the shell once again measured and inspected for damage.

**Results:** At a load of 630 lbf,  $0.65 \pm 0.1$  inches of deformation was measured across the monocoque. After unloading the shell, the fairing returned back to its original size, indicating that all deformation was elastic. The load-deformation curve was approximately linear, supporting the theory of that the deformation was elastic (Figure 20). A thorough inspection of the shell after the test revealed no delamination, cracked fibers, or other damage.

### Side Load

**Method:** The rollover protection system was tested with a 300 lbf side load applied at the shoulder. The monocoque was cantilevered from a steel structure clamped to the base of the seat (Figure 21a). No part of the vehicle other than the seat was supported.

Two team members with a combined weight of 325 lb stood on the vehicle and the deformation was measured (Figure 21b). The load was applied slowly, and the fairing was monitored for damage throughout the test. The two team members were fully supported

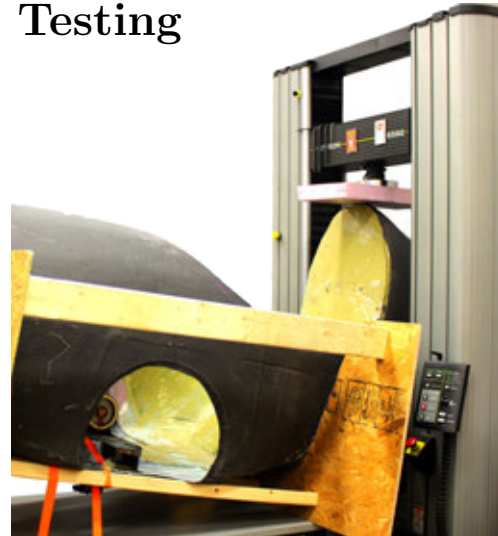


Figure 19: RPS top load test setup.

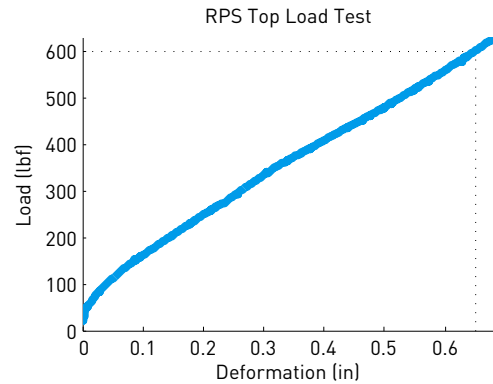


Figure 20: RPS top load force-deflection curve.

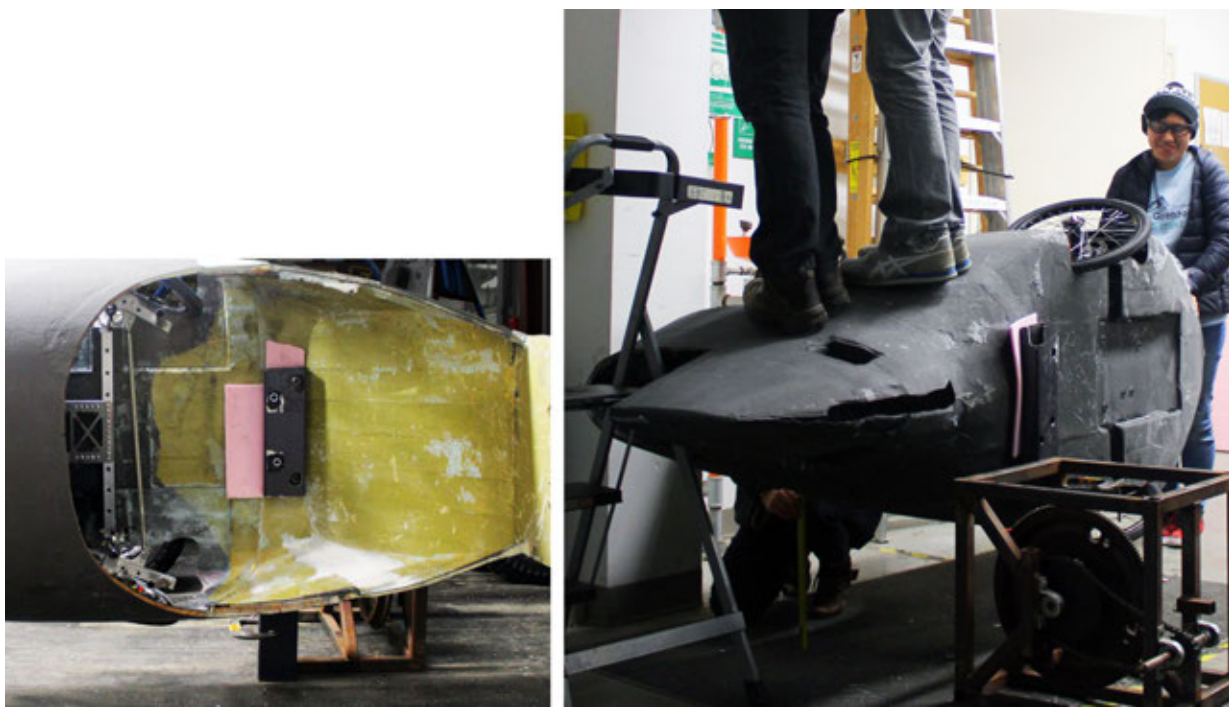


Figure 21: RPS side load constraint within monocoque (left) and test in progress (right).

by the side of the vehicle. After a final measurement and inspection, the load was removed.

**Results:** Under the 325 lbf load,  $0.38 \pm 0.2$  inches of deformation was measured at the shoulder with a tape measure. After unloading the shell, no non-elastic deformation was measured. A thorough inspection of the composite monocoque revealed no damage.

The test was performed twice with no measurable difference in deflection between the two trials. This gives the team confidence that the deformation was purely elastic and this load is well within the monocoque's load capacity.

## RPS Testing Conclusions

### Comparison to Specifications:

This testing verifies that *Llama Del Rey* meets both the RPS load specifications set forth by ASME and those outlined in the team's specification table.

	Load	Simulated Deformation	Measured Deformation	Difference
Top Load	600 lb	0.47 in	0.65 in	38%
Side Load	300 lb	0.32 in	0.38 in	19%

Table 7: RPS test/analysis comparison.

**Comparison to Analysis:** RPS test results were very similar to those predicted by the finite element analysis (Table 7). In both cases, the measured deformation was greater than the simulated deformation by less than 40%, a small difference considering that the simulation was performed assuming a completely isotropic and homogenous material.

**Design Modifications:** As the RPS met the team's product design specifications, no modifications were made to the design of the vehicle's rollover protection system.



## 16 Developmental Testing

### 16.1 Prone Position Testing

**Objective:** Determine if a prone rider position better achieves the team's goals.

**Method:** A rideable prone bicycle prototype was built by the team in the fall semester. The bicycle was tested for rider comfort and safety.

**Result & Impact on Design:** After testing the prone vehicle with multiple riders, the team felt that it did not support the goal of creating a bike that any team member can safely and practically ride. The aerodynamic advantage and ease of manufacturing did not outweigh safety concerns and the steep learning curve that could impede many team members from riding the vehicle. The prone vehicle design was not further pursued.

### 16.2 Automatic Shifting

**Objective:** Determine if an automatic transmission would benefit the vehicle's performance.

**Method:** The team developed and tested a prototype automatic shifting system. A Nu-Vinci continuously variable transmission (CVT) was coupled with a servo motor, sensors and a microcontroller to form the backbone of the system. A Hall Effect sensor measured rider cadence and the microcontroller shifted the transmission as needed.

**Results & Impact on Design:** Although a prototype was built and benchtop tested, the team was not able to conduct comprehensive road tests on the system before beginning the design of *Llama*. Furthermore, the CVT was substantially heavier than a traditional derailleur system. The team may perform additional testing on this system in future years.

### 16.3 Fairing Size Verification

**Objective:** Ensure *Llama*'s fairing is large enough to comfortably and safely fit all team members.

**Method:** A recumbent rider measuring jig was built. While riders sat on the jig, retroreflective spheres were swept over the rider volume and a three-dimensional point cloud was captured by an Opti-Track motion capture system (Figure 22). The test was performed by riders of different size.

**Impact on Design:** The generated point cloud was superimposed over the proposed fairing volume in SolidWorks. It was determined that all riders could comfortably fit into the vehicle, giving the green light for fairing manufacture to continue.

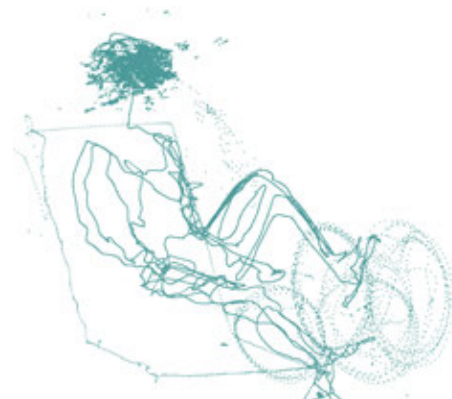


Figure 22: Generated rider point cloud.



## 16.4 Fairing Manufacturing Tests

**Objective:** Refine the fairing manufacturing process at small-scale before moving to large-scale manufacturing.

**Background:** The team has limited experience with male mold manufacturing which led to concerns about achieving an acceptable surface finish, easily removing the mold, and performing the process as a whole. Several tests were conducted to refine the process at small-scale before moving on to the full fairing.

**Surface Finish & Foam Removal:** A convex form was cut out of polystyrene foam with a CNC router. The shape contained complex curvature, much like that of the final vehicle. After applying carbon to the form, the surface finish was quantified by measuring surface height variation. The test resulted in a form with limited wrinkles, none more than 0.2" in height. Further testing demonstrated that the shape could be faired to result in an acceptable surface. Finally, the male mold was extracted to test ease of foam removal.

**Hatches:** A male mold with inset ribs was covered in carbon and its ribs filled with Nomex honeycomb. A hatch was cut from the form by slicing through the center of the ribs. The produced hatch was rigid and fit well into the base structure (Figure 23a,c).

**Window:** A one-third scale model of a potential head bubble design was constructed from solid plaster and sanded smooth. Several thicknesses of PET (.03", .04", .06") were vacuum formed over the mold and the optical clarity of the pieces was tested (Figure 23d). It was determined that acceptably clear finishes could be made with all plastic thicknesses.

**Full Process:** The full two-part male mold manufacturing process was tested in a series of lay-ups on a one-fifth scale model of the fairing (Figure 23b). The full process of mold preparation, carbon layup, rib filling, mold joining, and mold extraction was tested. This test confirmed the team's ability to build a structural fairing with a two-part male mold.

**Impact on Design:** These tests were instrumental in the design and refinement of the two-part fairing manufacturing process. As *Llama* is the team's first exploration into a structural CFRP monocoque built over a male mold, it was essential that the processes be tested before the construction of the main fairing.

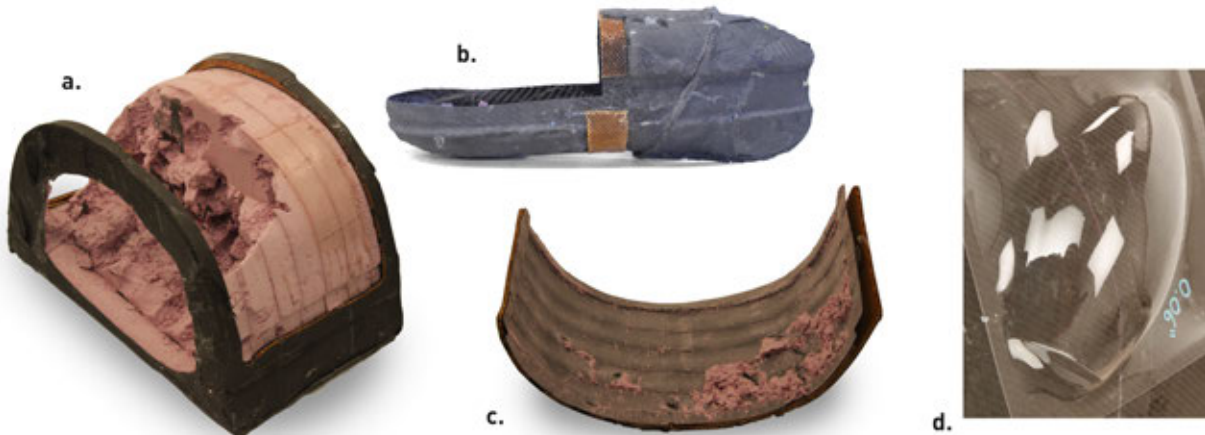


Figure 23: Fairing manufacturing tests.



## 16.5 Frame Structural Testing

**Background:** *Llama*'s front structural sub-frame is built from rectangular aluminum tube. Testing was done to evaluate methods of frame construction.

**Objective:** Determine the strength-weight tradeoff of welded and riveted structures.



Figure 24: Test samples and fixturing.

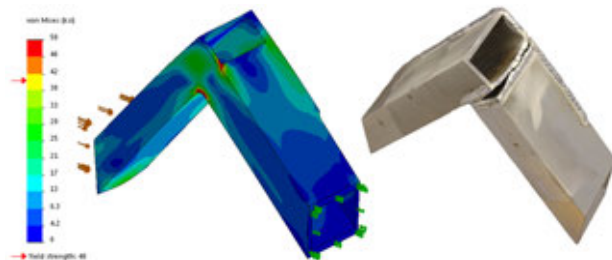


Figure 25: Welded structural test results.

buildup around the welds added enough strength to compensate for the lost temper.

The shear force applied on the failed 3/16" diameter rivets was calculated to be 475 lbs per rivet at failure. This exceeds the rivets rated shear strength of 310 lbs.

**Conclusions & Impact on Design:** Testing indicated that welded frames are at least 3x stronger than riveted frames. For the competition vehicle, the team will use welds for structural support and rivets to assist in weld jigging.

## 16.6 Rib Testing

**Objective:** Determine how many layers of carbon fiber and Nomex honeycomb must be applied to the monocoque to adequately protect the rider.

**Method:** Five variations of ribbing were subjected to 4-point bend testing to determine the modulus of elasticity for the ribs used in the fairing (Figure 26). The American Society for Testing and Materials recommends 4-point bend testing for determining the stiffness of sandwich laminates[1]. At least three



Figure 26: Rib test specimens.



specimens of each type of rib were tested.

For the purpose of calculating a useful modulus for analysis, the samples were assumed to be linear and isotropic. Beam bending equations were used to estimate the modulus of elasticity ( $E$ ) from the applied force ( $F$ ) and the measured deformation ( $\nu$ ) (Equation 3). Parameters in the formula include the x-coordinate of the left center support ( $a$ ), the x-coordinate of the right center support ( $b$ ), the distance between the outer supports ( $L$ ) and the bending moment of area of the section ( $I$ ).

$$E = \frac{-Fa}{6L\nu I} (aL^2 + bL^2 - 2a^3 - b^3 - ba^2) \quad (3)$$

All test samples were 1 inch wide. In addition to testing well-adhered test samples, several of the samples were intentionally poorly bonded to simulate potential weak areas of the monocoque. Modulus is a useful test metric as the data from these tests can be used for analysis of deformation at load (Section 10).

**Results:** The five rib sections were each tested and the modulus of elasticity was calculated from the linear region of their load-deformation curve (Table 8). The tests were stopped after the samples exhibited significant non-elastic deformation. Test samples failed either through delamination or cracked fibers.

Laminate Material	Core Material	Edges Bonded	Bond Quality	Modulus of Elasticity
2x 6K Twill Carbon	-	Yes	Good	$60 \pm 12$ GPa
2x 6K Twill Carbon	.5" Nomex Honeycomb	Yes	Good	$2.5 \pm 0.1$ GPa
6K Twill Carbon, Kevlar	.5" Nomex Honeycomb	Yes	Good	$1.3 \pm 0.1$ GPa
2x 6K Twill Carbon	.5" Nomex Honeycomb	Yes	Poor	$2.0 \pm 0.1$ GPa
2x 6K Twill Carbon	.5" Nomex Honeycomb	No	Good	$1.3 \pm 0.1$ GPa

Table 8: Rib test results.

Note that although the modulus values for the solid carbon without a honeycomb core are significantly higher than that of cored samples, the tested samples were thinner and more flexible than the honeycomb-cored samples.

**Statistical Analysis:** At least three samples were tested of each of the sections. Error was estimated as one standard deviation from the mean. Although standard deviation deflation typically occurs with small sample counts, it is usually minor. For most of the profiles, the test samples exhibited little deviation in modulus, validating the results.

**Conclusions:** While the samples tested are not as stiff as published values for CFRP laminates[2], they are representative of the construction of *Llama*'s fairing. It is notable that the testing suggests that poor laminate bonds only reduce the modulus by 20%, suggesting that a rib with an imperfect laminate is still quite stiff.

**Impact on Analysis & Design:** The results from the carbon/honeycomb well-adhered laminate samples tested were fed into the RPS analysis (Section 10) to predict the deformation of the fairing under load. Analysis suggested that the sections tested would be strong enough to adequately protect the rider. The small difference between the strength of well and poorly bonded sandwich laminates gives the team additional confidence in the fairing, as it will protect the rider even if the ribs are not perfectly bonded.



## 17 Performance Testing

### 17.1 Weight Testing

**Objective:** Test how *Llama*'s weight compares to the design specification and identify areas of opportunity for weight reduction.

**Method:** All parts of the vehicle were individually weighed and tabulated.

**Results & Error Analysis:** The total vehicle weight is estimated at 64 lbs (Table 9). Note that components were weighed in the granularity presented in the table and were not broken down to the smallest possible unit. The scale used was recently calibrated, but had a resolution of 0.5 lbs. Across the 12 weighings done, there is the possibility for stackup error of  $\pm 3$  lbs.

**Comparison to Design Specifications:** Testing indicates that the vehicle weight will be  $64 \pm 3$  lbs, on target with the 65 lb specification.

**Impact on Design:** Weight testing indicates that the best opportunities for weight reduction are in the front frame assembly, specifically the adjustable pedals and the steering. Lightening these assemblies will be investigated before competition. While the fairing shell represents more than half of the vehicle weight, it serves as the RPS and will not be changed.

### 17.2 Visibility Testing

**Objective:** Ensure that *Llama*'s field of vision allows for safe operation and meets the design specification.

**Method:** One team member of average size sat in the fairing, identifying the closest points on the ground that she could see around the vehicle while turning her head. As booster seats will be used to equalize rider height, only one test was necessary.

**Results:** The rider's field of view was determined to be  $240^\circ$ . The data from the test was used to create a visibility map (Figure 27).

Subsystem	Component	Weight (lbs)	
Fairing	Shell	28.0	33
	Main Hatch	3.0	
	Rear Hatch	2.0	
Front Frame	Frame	1.7	19
	Adjustable Pedals	6.5	
	Knuckles & Steering	6.8	
Rear Wheel	Wheels	4.0	3
	Shaft & Mount Plates	0.5	
	Wheel	2.5	
Misc.	Chain	4.0	9
	Seatbelt	2.0	
	Hardware	3.0	
Total		64	

Table 9: Vehicle weight estimate.

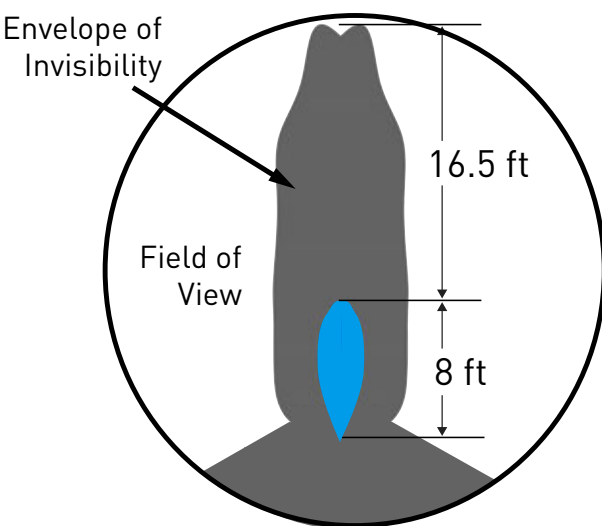


Figure 27: Visibility testing results.



**Comparison to Specifications:** The rider's  $240^\circ$  field of view exceeds the  $200^\circ$  design specification by 20%. Furthermore, the vehicle has a 60% wider field of view than *Cheryl's*  $150^\circ$ .

**Impact on Design:** Although *Llama* has excellent visibility, there is still a large blind spot behind the rider. Mirrors and other visibility features will be added to further increase the field of view.

### 17.3 Turning Radius

**Objective:** Ensure that *Llama* can turn within the radius outlined in the design specification.

**Method:** *Llama Del Rey's* steering was pushed to one extreme and the vehicle was moved in a circle. The arc of the outer wheel was marked on the ground in chalk and later measured. Half of the wheelbase width was subtracted from the chalk line radius to determine the centerline turn radius. Two tests were performed in each turn direction to ensure accuracy of results.

Measurement	Radius
Left Turn	2.44 m
Right Turn	2.31 m
Specification	3.00 m

Table 10: Turn test results.

**Results & Comparison to Specifications:** *Llama's* turning radius is slightly different in each direction of turn. Both the left and right turning radii are less than 2.45 m, 18% better than the 3 m specification (Table 10).

**Impact on Design:** After testing, the wheel cutouts in the monocoque will be widened to allow for equally tight turning in each direction.

### 17.4 Center of Mass

**Objective:** Ensure that *Llama's* center of mass is low enough to ensure stability while turning.

Vehicle	Position	Height
Llama Del Rey (2015)	24.5 in	15.6 in
Cheryl (2014)	33.4 in	17.1 in

Table 11: Center of mass location.

**Method:** *Llama* was tilted and balanced in two directions with a rider inside, and the intersections between the balance planes were used to locate the center of mass. The center of mass was assumed to be along the centerline of the vehicle. The center of mass is quantified as the distance from the rear wheel and the height above the ground.

**Results & Comparison with Analysis:** *Llama* has a slightly lower center of mass than *Cheryl* (Table 11). This lower center of mass will give *Llama Del Rey* additional rollover resistance when turning (Analysis Section 13.2).

### 17.5 Handling Testing

**Objective:** Ensure that *Llama's* steering is adjusted for prime handling performance.

**Method:** *Cheryl's* camber and toe-in were adjusted at the kingpins and steering tie-rods. The vehicle was adjusted to different handling settings and then ridden for a qualitative assessment by the rider.

**Results:** *Cheryl's* ideal camber was determined to be slightly negative, to optimize for straight-line efficiency and grip while cornering. The best toe-in setting was determined to



be neutral for high efficiency.

**Impact on Design:** *Cheryl's* tie rod adjustments were determined to be too coarsely spaced to be useful. The plates were modified accordingly and toe-in adjustment on *Llama Del Rey* is now performed with the axial threads on the tie rods.

## 17.6 Rider Changeover

**Objective:** Ensure that riders can enter the vehicle, adjust the pedals to their preferred position and be ready to ride in a reasonable amount of time.

**Method:** For various riders, the total time elapsed from entering the vehicle to finishing adjusting pedals was measured via stop watch.

**Results & Comparison to Specifications:** The total time elapsed during the pedal adjustment and vehicle entrance process was an average of 20 seconds for the three riders tested. This is well under the 60 second specification that the team allotted for rider switching during the endurance race. It is noted that the addition of seat belt adjustment and hatch application will add some time to the entire process, but the team is confident that these can be done in less than 40 seconds with the help of other team mates.

**Impact on Design:** Testing indicated that there should be marks on the adjustable pedals that indicate the different distance settings. These will be added before competition.

## Part IV

# Safety

## 18 Design for Safety

*Llama Del Rey* is the safest vehicle ever produced by Olin College's HPV Team. The largest safety risk, both to the rider and bystanders, is high-speed impact. *Llama* is specifically designed to avoid collisions, but is also capable of weathering them when they occur. *Llama* provides superior stability, vision, and visibility to reduce crash likelihood.

**Stable Configuration:** Stability comes in several forms. First, tricycles are inherently stable when stopped or moving at low speeds. Standard two-wheel recumbents often fall just after starting forward, especially with inexperienced riders. While these impacts are generally slight, they can leave the vehicle in the path of other vehicles and lead to severe secondary damage. *Llama's* stability also extends to operation at higher speeds. With improved stability over *Cheryl*, *Llama* will be capable of making evasive turns at any speed to avoid collision threats. Rollover Analysis (Section 13.2) was performed to give *Llama* an ideal wheelbase for stability. Finally, in the event of grip loss, the caster and toe-in angles used in the vehicle's Ackerman geometry will simply re-center the steering forward in a graceful, predictable, and safe recovery.

**Vision:** Whether riding with the clear aerodynamic windshield or without, *Llama* gives



an unobstructed forward view, critical to avoiding crashes (see Section 17.2). With an anti-fogging spray applied to the inside of the head-bubble, *Llama*'s riders will have excellent vision in all environmental conditions. Finally, the rider's eye level is 35" from the ground, 8.5" higher than with *Cheryl*, yielding better vision.

**Visibility to Others:** *Llama*'s color scheme has been designed to catch the eye not just for aesthetics, but also to maximize its safety. Between its bright paint scheme and 43" height, it will be hard to miss. Standard upright bicycle features including reflectors, white head lights, and red tail lights make *Llama* visible day or night.

**Rollover Protection System:** If a crash does occur, *Llama* is well equipped to minimize its impact on the rider within. First, the structural fairing is designed to reduce impact energy with its leaf-spring shaped forward section constructed of Nomex ribs and carbon fiber. This section of the fairing is expansive enough to compress significantly inward without impinging on the rider's volume. More significant impacts will meet the rollover protection system which ensconces the rider. This rollbar is tightly integrated into the fairing's ribbed structure and consequently will not shear or plastically deform under expected impact forces. All edges of the fairing have been rounded and there are no sharp points protruding to harm a rider. The seat and RPS have also been covered in Kevlar to limit any contact with carbon splinters in case of catastrophic failure.

**Collision Recovery:** The inherently stable tricycle design will keep the vehicle upright when experiencing light to moderate impacts. This quality is critical to making *Llama* safe in collisions. By remaining upright, the rider can recover quickly and pedal to a safe location, rather than being helplessly stuck in the event of additional approaching danger. Once a safe place is reached, the safety harness, which keeps the rider safely constrained within the vehicle, can be quickly released. In the case of a moving collision where the rider releases the steering handles, the steering geometry configuration naturally returns to center rather than making violent, uncontrolled course corrections. To further protect the rider, hand-guards were implemented into the steering tiller to avoid contact with moving components in the event of a collision. These hand guards cover the rider's fingers and knuckles, while still allowing clear access to the brake levers. Should the vehicle be inverted in a collision, the rider will still be able to exit quickly through the main hatch. If the rider is rendered unconscious in an incident, first responders will be able to quickly remove the hatch and release the safety harness to extract the rider. Because the hatch is constrained using integrated magnets, it can be opened from the outside with ease.

**Bystander Safety:** As a final safety design consideration, *Llama* was made to minimize the likelihood and impact of collisions with bystanders. Good rider vision and vehicle visibility will allow riders to avoid bystanders and bystanders to avoid *Llama* respectively. The addition of a bell also aids the rider in warning bystanders of *Llama*'s imminent approach. In the unfortunate case of a collision, *Llama*'s smooth, rounded surfaces will minimize damage to the bystander.



## 19 Hazard Analysis

Hazards accompany any mechanical system. For both the safety of the rider and the overall performance of *Llama*, a list of possible hazards are examined and identified. Solutions or temporary fixes that keep the system running and the rider safe are presented (Figure 28).

Likelihood	Hazard	Planned Mitigation
High	Window fogs up	NACA duct in fairing directs air flow at rider and window. An anti-fog spray is used as a preventative measure.
	Rider overheats	The head bubble is easily removed from the inside or outside and fresh air is accessible. As a preventative measure, air ducts have been incorporated.
	Rider needs to stop suddenly	Disk brakes can quickly stop vehicle.
Medium	Flat tire	Apply brakes and replace parts at pit stop.
	Rider gets dehydrated	A hydration bladder is available and can be stored inside the vehicle.
	Rider loses grip on handles	The steering geometry configuration is self correcting and will straighten the vehicle's trajectory, making it easy for the rider to regain control.
	Broken chain	Run vehicle to pit stop and necessary repairs will be made. The chain is routed under the vehicle, making it easy to access and repair.
	Vehicle crash or rollover	Sturdy RPS, carbon fiber fairing, and extra ribbing in weak spots protect rider. Fairing can be opened from inside or outside.
	Undesired road conditions or high traffic area	The head bubble has a large field of view and riders are experienced with vehicle operation.
	Loose or damaged part on vehicle	Run vehicle to pit stop and necessary repairs will be made with available tools.
	Unattended vehicle rolls away	Wheel blocks and brake lock on handlebars.
	Wet conditions on track	Riders are well-trained in Boston weather and vehicle is very stiff, giving good road feel.
	Glare interferes with rider	Wear sunglasses. Head bubble is removable.
Low	Tie rod breaks	Rollover protection system protects rider in case of loss of control. Dual disk brakes can quickly stop vehicle.
	Rider cannot fit in vehicle comfortably	Vehicle is designed for a wide range of rider sizes with an adjustable pedals swing arm, and booster seats.
	Steering stuck	Disk brakes quickly stop vehicle for maintenance.

Figure 28: Hazard analysis and mitigation.

## 20 Safety in Manufacturing

Safety is not only a priority during vehicle use, but also during the manufacturing process. When working in the machine shop, team members are mandated to tie back all hair and loose clothing, long pants are worn with closed-toed shoes, and safety glasses are worn at all times. Proper ventilation and fume extractors are used while welding, as well as proper protection for eyes and skin. All team members working with metalworking tools are trained for proper use by machine shop supervisors and have passed the required safety tests set by Olin College.

When working with composite materials, safety glasses, gloves, and respiratory protection are worn to protect team members from dust, fiber, and fumes. The team makes



a conscious effort to choose the safest epoxy available to limit possible inhalation and skin-contact risks. The team also works to limit particulates released by minimizing the amount of sanding and cutting of the CFRP laminate. The team decided not to dissolve the polystyrene foam and use minimal hot wire cutting to reduce team members' exposure to the harmful fumes produced by these operations.

During all work times, no team member is allowed to work alone, which limits the chance of injury and encourages all team members to make safer decisions together. In the case of an emergency, the second team member would be able to assess the situation and take the appropriate actions.

## Part V

# Conclusion

## 21 Comparison

Experimental results and analytical predictions are compared to design specifications in Table 12. All quantitative targets were directly compared to the analytical and experimental results where appropriate. Qualitative metrics were evaluated by comparison to previous vehicles.

Specification	Target	Analytical Prediction	Experimental Result	Target Met?
Roll bar vertical strength	600 lbf	> 600 lbf	> 630 lbf	✓
Roll bar lateral strength	300 lbf	> 300 lbf	> 325 lbf	✓
Turning radius	3 m	3.0 m	2.4 m	✓
Weight	65 lb	-	64 lb ± 3 lb	✓
Vehicle construction time	350 hrs	-	350 hrs	✓
Vehicle width	32 in	-	31.0 in	✓
Vehicle length	92 in	-	94.7 in	x
Drag coefficient ( $C_dA$ )	0.05	0.053	-	x
Cost of materials	\$2,500	-	\$2,770	x
Field of View	200°	-	220°	✓
Number of parts	50	-	56	x
Cargo area can fit grocery bag	Yes	-	Yes	✓

Table 12: Specification comparison.

## 22 Evaluation

The majority of *Llama Del Rey's* design specifications were met and are discussed below:

- Rollover protection system analysis and testing demonstrated that the rollbar supports the required load with minimal deflection.
- Vehicle turning radius was found to exceed expectations, set by the Ackerman steering simulation used during design, by 20%.



- Although final weight has yet to be determined, subsystem-level testing indicates that the vehicle will hit its target weight specification.
- Vehicle construction time was reduced to the target of approximately 350 man hours.
- Vehicle length and width were measured to be similar to target values. Although the vehicle is slightly longer than intended, this should not affect its transportability.
- Analytical simulations suggest a drag coefficient 6% worse than the target value.
- Accounting methods were used to keep track of material costs during the fabrication process, yielding a final expense excess of 10.8%.
- The measured field of view exceeds the target value by 10%.
- The number of machined parts exceeds the target by 12%, but was a significant reduction over the previous year's 66 parts. Manufacturing labor was successfully reduced.
- Grocery bag fitting was determined by inserting a grocery bag (of the size specified by ASME HPVC) into the vehicle's cargo area and replacing its covering hatch.

Some of the design specifications can not be evaluated at this time. These include: drivetrain efficiency, repair time, stopping distance, handling response, rider safety harness presence, lack of sharp edges, and vehicle aesthetics. These qualities will be collected once the vehicle is closer to finalization. Final specification comparison will be presented in the design update presentation.

## 23 Recommendations

More work could be put into increasing *Llama*'s practicality and refining the overall design. Further steps could be taken to reduce the vehicle's total weight, increasing acceleration and facilitating hill climbing. Most significantly, a revised fairing could be produced with unidirectional carbon fiber optimally applied across the rib structure, yielding similar strength with reduced weight. Less drastically, aluminum frame tubes could be replaced with carbon members and material could be removed from several parts for a reduced factor of safety.

Electronic subsystems could be installed within *Llama* to quantify and assist the rider's performance. Rider heart rate, pedaling cadence, wheel speed, and vehicle angle could collectively feed data into a battery-based electric motor assist system, which would help the rider climb hills. Regenerative braking and anti-lock brake schemes could also be explored. Aesthetically, *Llama* could be finished with an Automotive Class A paint job and a surface perfecting wax. Were *Llama Del Rey* to be mass produced, additional effort would be required to reduce the labor needed to produce its parts. Specifically, the molding method might be reconsidered, as a multi-use female mold could reduce production labor requirements.

Many of these improvements will be pursued in future years. The team is excited about the progress made this year and proud to present *Llama Del Rey* at the ASME 2015 Human Powered Vehicle Challenge West.



## References

- [1] ASTM, 2006 (2012), “Standard Practice for Determining Sandwich Beam Flexural and Shear Stiffness”, D7250.
- [2] Engineering Toolbox, 2014, “Modulus of Elasticity for Common Materials,” Web.
- [3] Friction Facts, 2014, “Friction Facts Efficiency Report Package,” Boulder, CO.
- [4] Industrial Fasteners Institute, “Fastener Ultimate Tensile Strength Explained,” Independence, OH.
- [5] Olin College Human Powered Vehicle Design Team, 2014, “Cheryl,” Needham, MA.
- [6] Gribble, S., n.d., “Interactive Cycling Power and Speed Calculator,” Web.
- [7] Horowitz, R., 2010, “The Recumbent Trike Design Primer,” Lago Vista, TX.
- [8] Tufts University Future Technologies Lab, “Friction Testing,” Medford, MA.
- [9] University of Toronto Human Powered Vehicle Design Team, 2014, “Valkyrie,” Toronto, ON.
- [10] Aird, F., 2006, *Fiberglass and Other Composite Materials*, Penguin Publishing Group, New York, NY.
- [11] Beauchamp, W., 2000, “Barracuda Fairing Phase 3,” Web.